



Evaluation of convection-permitting WRF CONUS simulation on the relationship between soil moisture and heatwaves

Zhe Zhang¹ · Yanping Li¹ · Fei Chen² · Michael Barlage² · Zhenhua Li¹

Received: 30 December 2017 / Accepted: 15 October 2018 / Published online: 24 October 2018
© Springer-Verlag GmbH Germany, part of Springer Nature 2018

Abstract

Soil moisture plays an important role in modulating regional climate from sub-seasonal to seasonal timescales. Particularly important, soil moisture deficits can amplify summer heatwaves (HWs) through soil moisture-temperature feedback which has critical impacts on society, economy and human health. In this study, we evaluate decade-long convection-permitting Weather Research and Forecast (WRF) model simulations over the contiguous US on simulating heatwaves and their relationship with antecedent soil moisture using a dense observational network. We showed that the WRF model is capable of capturing the spatial pattern of temperature threshold to define HWs, though the simulation shows a warm bias in the Midwest and cold bias in western mountainous regions. Two HW indices, based on frequency (HWF) and magnitude (HWM), are evaluated. Significant anti-correlations between antecedent soil moisture and both HW indices have been found in most parts of the domain except the South Pacific Coast. A detailed study has been conducted for the Midwest and South Great Plains regions, where two heatwaves had occurred in the last decade. In both regions, the high quantile of the HWF distribution shows a strong dependence on antecedent soil moisture: drier soil leads to much larger increase on the upper quantile of HWF than it does on the lower quantile. Soil moisture effects on the higher end of HWM are not as strong as on the lower end: wetter antecedent soil corresponds to a larger decrease on the lower quantile of HWM. WRF captures the heterogeneous responses to dry soil on HWF distribution in both regions, but overestimates these HWM responses in the Midwest and underestimates them in the South Great Plains. Our results show confidence in WRF's ability to simulate HW characteristics and the impacts of antecedent soil moisture on HWs. These are also important implications for using high-resolution convection-permitting mode to study the coupling between land and atmosphere.

Keywords Soil moisture · Heatwave · Regional climate · Land–atmosphere interaction · Soil moisture-temperature feedback · WRF

This paper is a contribution to the special issue on Advances in Convection-Permitting Climate Modeling, consisting of papers that focus on the evaluation, climate change assessment, and feedback processes in kilometer-scale simulations and observations. The special issue is coordinated by Christopher L. Castro, Justin R. Minder, and Andreas F. Prein.

✉ Yanping Li
yanping.li@usask.ca

¹ Global Institute for Water Security, University of Saskatchewan, Saskatoon, SK, Canada

² National Center for Atmospheric Research, Boulder, CO, USA

1 Introduction

Summer heatwaves (HWs) have significant impacts on the environment, society, and human health (Brooke Anderson and Bell 2011). Under climate change, these extreme hot events are projected to become more frequent, intense and longer (Meehl and Tebaldi 2004; Diffenbaugh and Ashfaq 2010; IPCC 2012). Thus, understanding the physical mechanisms of HWs and improving HW forecast skills is of great importance and allows a proactive approach to mitigating potential HW damages.

Although persistent synoptic high pressure induced by large scale atmospheric blocking is a necessary factor in causing persistent heatwaves (Perkins 2015), land–atmosphere interactions also play an important role in amplifying the hot extremes through a soil moisture-temperature

feedback mechanism (Jaeger and Seneviratne 2011; Miralles et al. 2014). Soil moisture availability determines the evapotranspiration, a key process in exchange of water and energy between the land surface and atmosphere. During dry periods, low soil moisture limits the available surface energy converted to latent heat. More energy is partitioned as sensible heat flux, inducing an increase of near-surface temperature. Increased temperature then leads to a higher vapor pressure deficit and evaporative demand, and thus to a potential increase in evapotranspiration despite the already existing dry conditions, leading to a further soil desiccation (Seneviratne et al. 2010).

The soil moisture-temperature feedback mechanism and its impacts on heatwaves have been studied using climate models both in long-term climate simulations (Koster et al. 2004, 2006, 2009; Guo et al. 2006; Seneviratne et al. 2006; Jaeger and Seneviratne 2011) and regional events studies (Fischer et al. 2007; Whan et al. 2015; Hauser et al. 2015). Both studies contribute to our understanding of the feedback mechanism and the key role that soil moisture plays to influence near-surface temperature. However, these results, by perturbing initial soil moisture or decoupling the land from the atmosphere, could be artificial and model-dependent. Substantial observational evidence is needed to further understand the soil moisture-temperature feedback.

Several observations have confirmed previous modeling studies at regional (Durre et al. 2000; Hirschi et al. 2011; Quesade et al. 2012; Meng and Shen 2014; Sun et al. 2017) and global scale (Mueller and Seneviratne 2012). These works focus on the relationship between antecedent precipitation/soil moisture and summer hot extremes, and its impacts on different distributions of hot extreme indices. Owing to the lack of extensive long-term soil moisture observations, they inferred soil moisture conditions using a precipitation based index called the standardized precipitation index (SPI) (McKee et al. 1993). Their results showed that antecedent negative soil moisture anomalies were associated with a high frequency of summer hot day as well as longer duration of HW. Although precipitation is a major driver for soil moisture, SPI does not consider the effect of evapotranspiration. A similar multi-scalar statistical index called the standardized precipitation evapotranspiration index (SPEI) has been proposed to account for both precipitation and evapotranspiration on soil moisture (Vicente-Serrano et al. 2009).

Although the above observational studies have shown evidence of soil moisture-temperature feedback on HWs, they mainly focused on the frequency and duration of HWs, while the HW intensity and its relationship with soil moisture has not yet been assessed. A statistical significant correlation suggests a strong connection between soil dryness and extreme heat, but does not necessarily imply causality (Mueller and Seneviratne 2012). Moreover, previous regional climate model

simulations could capture the link between the soil moisture deficits and hot extremes but only for the moisture-limited regime. For wetter climates, the models tended to overestimate the strength of soil moisture-temperature feedback (Hirschi et al. 2011). Furthermore, previous studies used data from both global/regional models and gridded observational/re-analysis products at a spatial resolution of 50–100 km, which is not sufficient to capture the land–atmosphere feedback and perform HW impact studies on a local scale.

Long-term climate downscaling using convection-permitting models (CPM) provides an opportunity to fill the gaps in spatial scales (Prein et al. 2015). A 13-year (2000 October–2013 September) 4-km CPM simulation was conducted for the contiguous US (CONUS), using the Weather Research and Forecast (WRF) model (Liu et al. 2017). The CPM simulation, by explicitly resolving convection, improves summer precipitation simulations (Liu et al. 2017), which is important for assessing soil-moisture evolution and land–atmosphere feedbacks. This simulation represented realistically fine-scale land surface properties, such as topography and land-cover types which are critical in land–atmosphere coupling studies. In addition, the fine resolution dynamical downscaling allows the studies of HW impacts on local scale, which is more relevant to public health issues.

The purposes of this study are to: (1) evaluate different temperature thresholds in defining the simulated HW for two HW indices; (2) assess the correlation between antecedent soil moisture and summer HWs in the WRF CONUS simulation; and (3) evaluate how differently the distribution of HW indices responds to observed soil moisture and how well this feature is represented in the WRF 4-km CONUS simulations. The Midwest (MW) and South Great Plains (SGP), where soil moisture-temperature feedbacks are strong and two extreme heatwaves happened in 2006 and 2011, are investigated in detail. This paper is organized as the following: Sect. 2 describes observation and WRF simulation datasets, as well as the indices used to define heatwaves and soil moisture anomaly; Sect. 3 evaluates the CPM WRF in simulating HWs and discusses their correlations with antecedent soil moisture against observation datasets; Sect. 4 provides a broad discussion of antecedent soil moisture as a physical driver of HWs, its predictive skills and WRF CONUS performance compared to observation and other studies; conclusions are provided in Sect. 5.

2 Data and methods

2.1 WRF model

Previous studies have stated the advantages of high resolution convection-permitting modeling in studying the land

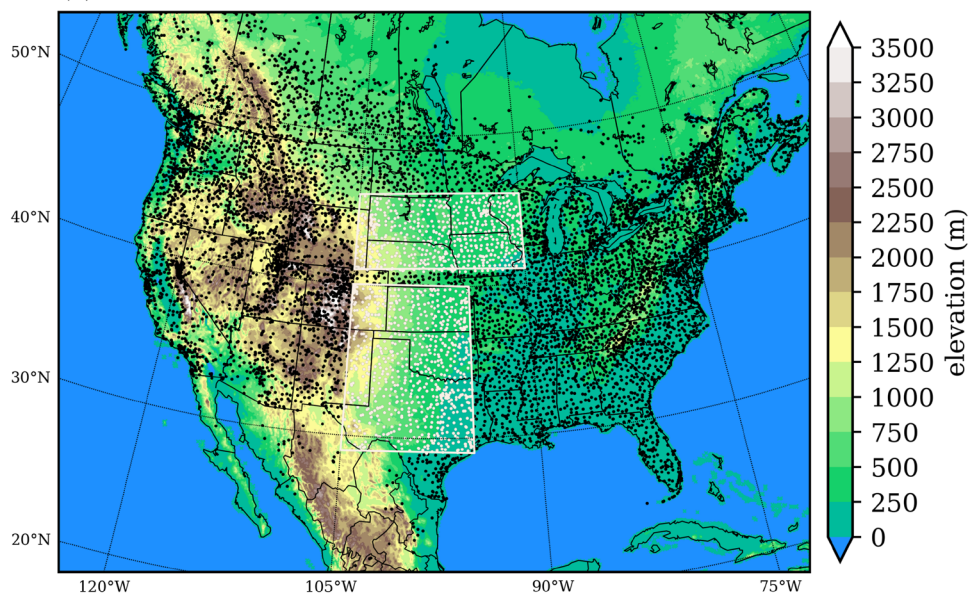
surface processes, by improving the representation of fine-scale terrains, such as mountainous and urban areas, and the heterogeneity of surface fields, such as soil moisture (Prein et al 2013a, b, 2015). In this study, we use high-resolution convection-permitting regional climate simulations, conducted on the Weather Research and Forecasting (WRF) model V3.4.1 (Skamarock et al. 2008), to explore the soil moisture-temperature feedback on summer HWs. The simulations start from the October of 2000 and run to the September of 2013 on 4-km horizontal grid spacing (1360×1016 grid points), covering the contiguous US (CONUS) (Fig. 1a). The physical parameterization schemes

used in these simulations are the Thompson aerosol-aware microphysics (Thompson and Eidhammer 2014), the Yonsei University (YSU) planetary boundary layer (Hong et al. 2006), the rapid radiative transfer model (RRTMG; Iacono et al. 2008) and the Noah-MP Land Surface Model (LSM). (For more detailed descriptions about the selection of physical schemes, model modifications, and simulation configuration, please see Liu et al. 2017).

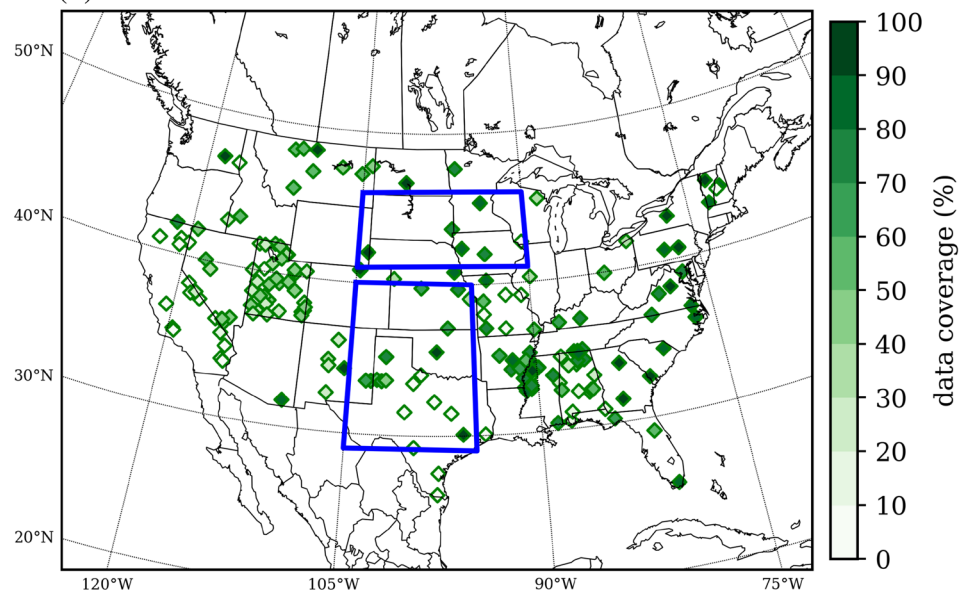
In the CONUS WRF simulations, soil moisture and surface fluxes exchange to the atmosphere are simulated by the Noah-MP Land Surface Model (LSM) (Niu et al. 2011; Yang et al. 2011), a community model with multi-parameterization

Fig. 1 **a** WRF model domain (5440 km × 4064 km) at 4 km grid spacing showing topographic elevation in meters. Black dots are the locations of observational stations of GHCN meteorological network (9877 within model domain). Stations within the white boxes are located in Midwest and South Great Plains and are selected for the regional study. **b** Locations of soil moisture measurement from SCAN (185 within model domain) and their data availability within our simulated period;

(a) WRF CONUS terrain and station location



(b) USDA SCAN site location



options to the original Noah LSM (Chen and Dudhia 2001). The Noah-MP LSM has been applied broadly, both in offline mode (Cai et al. 2014a, b) and coupled with atmospheric models (Chen et al. 2014; Barlage et al. 2015). Particularly, previous studies have shown improvement in simulating snowpack (Musselman et al. 2017) and severe storm forecast (Duda et al. 2017) by a more realistic representation of surface physics in the Noah-MP LSM coupled with high resolution CPM. In addition, Liu et al. (2017) provided several key modifications to the Noah-MP LSM, including microphysics-based snow-rain partitioning, realistic surface snow coverage representation, patchy snow in surface energy balance calculation, and heat transport by precipitation into the ground (see Liu et al. 2017). In this study, we are interested in soil moisture anomaly and how it contributes to summer HWs through soil moisture-temperature feedback. For this purpose, the WRF model simulated soil moisture anomalies are compared with an observational network (see Sect. 2.2) and the evaluation results are shown in Sect. 3.1.

2.2 Observations

To evaluate the WRF model temperature and soil moisture output, we used meteorological station data from the Global Historical Climatology Network-Daily dataset (GHCN-Daily) (Menne et al. 2012; Newman et al. 2015). Daily maximum temperature (T_{\max}) and precipitation data from a total number of 9877 stations within the WRF model domain are used to calculate heatwave indices and soil moisture proxy in this study. The locations of the GHCN-Daily station are also shown in Fig. 1a, with stations in the Midwest (MW, 41–46N, 90–105W) and the South Great Plains (SGP, 29–40N, 95–105W) are highlighted.

Soil moisture observations from the US Department of Agriculture (USDA) Soil Climate Analysis Network (SCAN) (Schaefer et al. 2007) are used to evaluate the simulations. The SCAN soil moisture data are collected by dielectric constant measuring devices at five different depths: 5 cm, 10 cm, 20 cm, 50 cm and 100 cm. The monthly top 1-m SCAN soil water content are integrated for each observation site and compared with the 1-m soil water integrated from the top three model soil layers (i.e., 5 cm, 25 cm, 70 cm) in Noah-MP. Due to measurement maintenance and data quality control issue, data from many stations are missing in various time, thus we calculated the ratio between available data (in monthly interval) and total period of simulation (from 2000 Oct to 2013 Sep) as the data availability. Figure 1b shows the locations of SCAN soil moisture measurement and their data availability within our simulation period.

To compare with observations from both SCAN and meteorological stations, the closest model grid points to the station locations are extracted. The fine grid spacing of the convection-permitting WRF model and the dense observational

network together allow the grid-to-station comparison between WRF model grid points and observational stations. In the following text, the analysis and variables derived from observation (including SCAN soil moisture and calculated temperature and soil moisture index) and WRF model are denoted as OBS and WRF, respectively.

2.3 HW indices

In this study, we apply the HW definition by Perkins and Alexander (2013), in which heatwave is defined as a consecutive period of extreme high temperature upon a statistically based threshold. In their definition, the threshold is the 90th percentile of daily T_{\max} for each calendar day in a year, TX90. This threshold is calculated based on a 15-day moving window, which is centered on the day in question, in order to account for seasonal cycle and obtain sufficient sample size for a realistic percentile value. The HW event is defined as three or more consecutive days when daily T_{\max} exceeds the TX90 threshold. Based on this definition, two HW indices, frequency and magnitude, are defined: HWF (heatwave frequency) is the number of days qualified as HWs and HWM (heatwave magnitude) is the mean daily T_{\max} during the HWs. For assessing soil moisture impacts on summer HWs, we calculated the TX90 threshold for each day in June–July–August (JJA) for the whole 13-year simulation period (during 2000 and 2013). Therefore, the two HW indices are obtained for these three months separately, in total 39 samples in 13 years.

2.4 Soil moisture indices

Because of the uncertainties inherent to long-term gridded soil moisture data, many studies have used different indices to estimate soil moisture deficit (Dai 2011; Hirschi et al. 2011; Muller and; Seneviratne 2012; Quesade et al. 2012). In this study, two hydro-meteorological indices were evaluated for model simulation and observational networks, including the soil moisture anomaly (SMA) and the standardized precipitation evapotranspiration index (SPEI).

The SMA describes the deviation of soil moisture in a period of a year to the soil moisture climatology and normalized by the standard deviation of soil moisture over the same period. In this study, the monthly top 1-m SMA is calculated from both the SCAN measurements and the closest grid points in WRF model, following the method of Orlowsky and Seneviratne (2013):

$$\text{SMA} = \frac{\bar{\theta} - \mu}{\sigma},$$

where $\bar{\theta}$ is monthly-averaged top 1-m soil water content, μ and σ are the mean and standard deviation of top 1-m soil moisture of the same months over the 13-year study period.

As shown in Fig. 1b, there are limited number of soil moisture measurements from SCAN network within the contiguous US domain. Only 185 stations have long term soil moisture measurement, while 9877 stations have temperature and precipitation observations. In order to get better coverage of soil moisture estimate, we used the SPEI index by Vicente-Serrano et al. (2009) to estimate the soil moisture anomaly in spring. The SPEI is based on precipitation and temperature data to calculate the accumulation of water deficit/surplus, precipitation minus potential evapotranspiration (P-PET), for a selected time period. Mathematically, the SPEI is similar to the SPI, but it also includes the effect of temperature variability on soil moisture deficit. The procedure proposed by (Vicente-Serrano et al. 2009) was used to estimate potential evapotranspiration by Thornthwaite's method (Thornthwaite 1948). And the P-PET series is fitted to a 3-parameter Pearson III distribution at each station to obtain the SPEI for both station observation and the WRF model. Here, the analysis focuses on the SPEI calculated on 3-month timescale (SPEI-3) to represent the seasonal soil moisture anomalies in spring. The values of SPEI represents the standard deviation from the mean state (0), where SPEI values larger/smaller than 0.5/− 0.5 represent abnormal wet/dry conditions.

2.5 Methodology

The analysis was conducted locally for each individual station and model grid point. For the evaluation of WRF simulation against observation, the model grid points that are closest to station locations were extracted. In this study, the relationship between two HW indices from the three summer months (June–July–August, JJA) and the spring soil moisture from preceding months (based on the 3-month SPEI described in Sect. 2.4), for the year 2000–2013. We applied three types of analysis on the monthly HW indices and soil moisture estimate.

First, the WRF model performance on simulating summer HW indices and soil moisture proxy were evaluated against meteorological station data and SCAN soil moisture measurements. For temperature evaluation, the model simulated TX90 threshold and HWF, HWM indices are compared to those derived from observation for the summer months (JJA). For the evaluation of model simulated soil moisture indices, the monthly SMA and the SPEI-3 timeseries are calculated from model output and compared with observation data from the SCAN.

Second, the HW indices for each summer month are related to their antecedent 3 months SPEI by calculating the Pearson correlation coefficient. The purpose of calculating correlation coefficient is to identify strong and significant correlated regions, as well as to evaluate model performance across the domain. Based on the correlation

coefficient results, regions with strong coupling between land and atmosphere can be identified.

Third, a quantile regression analysis was conducted to understand how soil moisture deficits impact the two HW indices. The ordinary linear regression shows the relation between the mean of the dependent variable y to the independent variable x . Quantile regression examines how different parts of the distribution of a dependent variable y respond to an independent variable x , based on the quantiles of choice. Special interests were focused on two regions, Midwest and South Great Plains, where two exceptional HWs had occurred in the last decade. The quantile regression of HW indices against antecedent SPEI are calculated for these two regions, and their regression slopes for each quantile are evaluated between the simulations and observations.

3 Results

3.1 Evaluation of WRF-simulated heatwave indices and soil moisture indices

The JJA seasonal averaged daily TX90 threshold from observation, WRF and their difference (model minus observation) are shown in Fig. 2. TX90 varies greatly across the contiguous US, with the hottest region in the Southwest desert area in Arizona exceeding 44 °C. Another extraordinarily hot region is located east of the Rocky Mountains in the South Great Plains, including Texas, Oklahoma, Kansas, Louisiana and Mississippi, with the threshold temperature higher than 40 °C.

The WRF simulation accurately captures the spatial pattern of the TX90 threshold, with two hot regions aforementioned and one cold region in the North and mountainous area. Figure 2c shows the difference of TX90 between WRF and observation, revealing a warm bias pattern straddled along the western edge of the Great Plains. For many global and regional climate model (Ma et al. 2014; Whan and Zwiers 2016), the summer warm bias is a common issue in near-surface temperature simulation over central North America for both mean and maximum temperature. The highest warm bias is about 3–4 °C in the Midwest and North Great Plains, mostly in Iowa, Nebraska, Minnesota and South Dakota. A noticeable cold bias of about 2–3 °C appears in the mountainous and valley regions west of the Rocky Mountains.

HWF characterizes the average number of HW days in a month, which is well simulated in WRF (Fig. 3b). However, WRF underestimates the spatial extent of the number of days contributing to HWF in the Midwest, Ohio Valley, Mississippi Basin, East Coast, and around the Great Basin.

The HWM is an index depicting the average magnitude of daily Tmax among HW days, which is identified based on

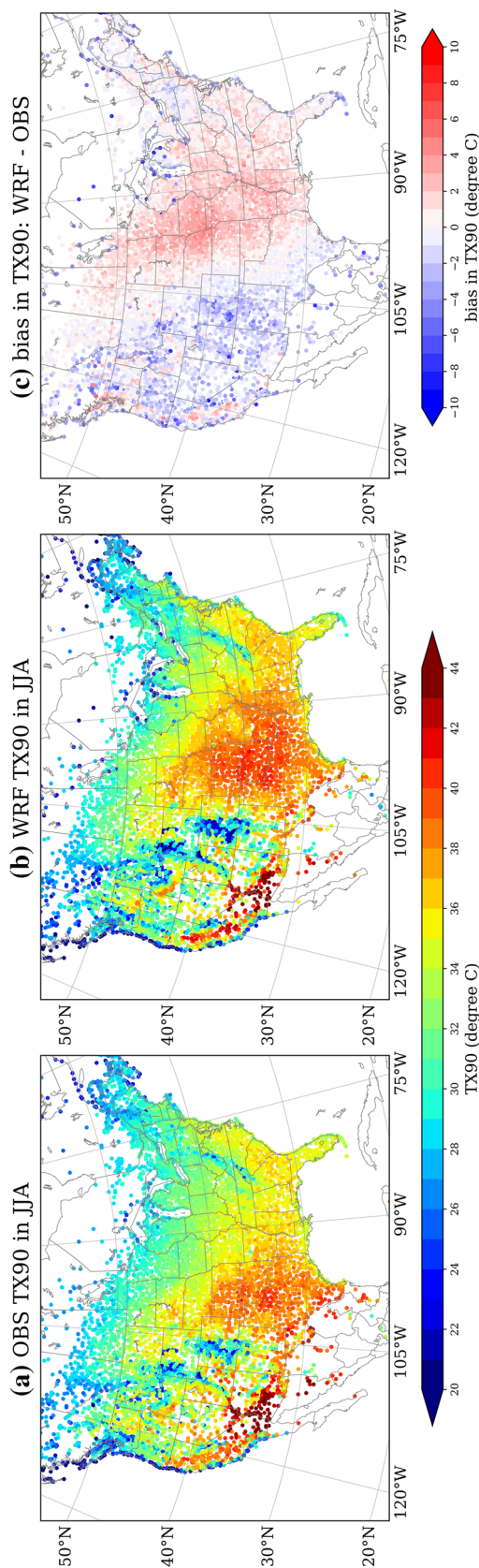


Fig. 2 JJA-averaged daily TX90 threshold temperature calculated for **a** station, **b** WRF model, and **c** model bias (WRF-OBS) for the summers of 2000–2013

the threshold temperature TX90. We show the HWM minus the TX90 threshold (HWM – TX90) in Fig. 3d–f. (HWM – TX90) can also be considered as an indicator of the variability of daily Tmax beyond its 90th percentile threshold. Both observations and WRF (Fig. 3d, e) show a larger magnitude (≥ 2 °C) in the northern part of domain (north of 40°N), and near both east and west coast in daily Tmax. But in the southern part of the domain, the departure of HWM to TX90 are generally small. This may imply a heavier tail in the distribution of daily Tmax for the northern part than the southern part of the domain. The WRF model captured correctly this feature with small difference (less than ± 1 °C). Overall, the HW threshold and HW simulated by the WRF CONUS simulation are reasonable in representing the observations and can be trusted in further analysis.

For soil moisture evaluation, the simulated top 1-m soil moisture anomaly from WRF model is compared with the SCAN measurement. The timeseries of monthly soil moisture anomaly for two selected regions (MW and SGP) are shown in Fig. 4. Since determining if the SPEI can represent soil moisture anomaly is of interest in these two regions, the SPEI-3 calculated for each month using meteorological data and WRF simulation are shown in dashed lines. The Pearson correlation coefficients between two soil moisture proxies, SMA and SPEI-3, from observation (OBS) and WRF model are shown in Table 1, with bold numbers indicating statistical significance ($p < 0.01$). In general, WRF model well captured the temporal variability of soil moisture anomaly accurately in both regions, with high correlation and statistical significance. SPEI is a good indicator for soil moisture anomaly, with higher correlation in SGP than in MW. The SPEI-3 derived from WRF model in both regions are in good agreement with that from observation, thus it is reasonable to use SPEI-3 as a soil moisture indicator and WRF model has accurately simulated this index.

3.2 Correlation between heatwaves and antecedent soil moisture

To determine the statistical relationship between antecedent soil moisture represented by SPEI-3 and the HW indices used in this study, we calculated their Pearson correlation coefficients over the 13-year period (Fig. 5). Significant anti-correlations with SPEI-3 exist for both HWF and HWM ($p < 0.01$) and appear in most regions in the continent, except for the Southwest region of the Pacific coast. The significant regions in HWM are generally further east compared to those in HWF, both in the observation and WRF. These anti-correlations suggest dry (wet) springs are associated with more (less) HW days and higher (lower) HW temperature in summer months.

The WRF model accurately captures these significant anti-correlations between antecedent soil moisture and

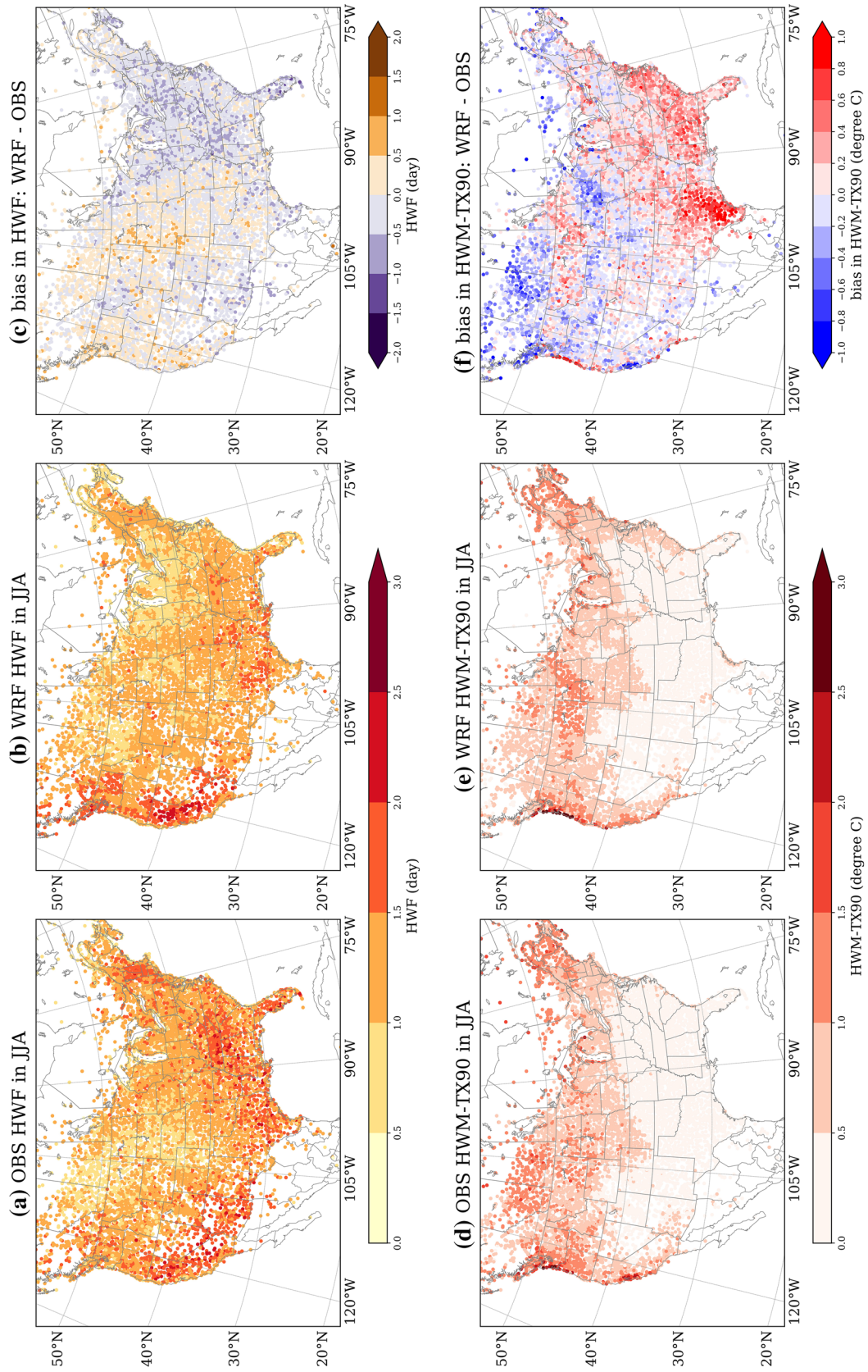


Fig. 3 Same as Fig. 2 but for HWF (a–c) and (HWM-TX90) (d–f)

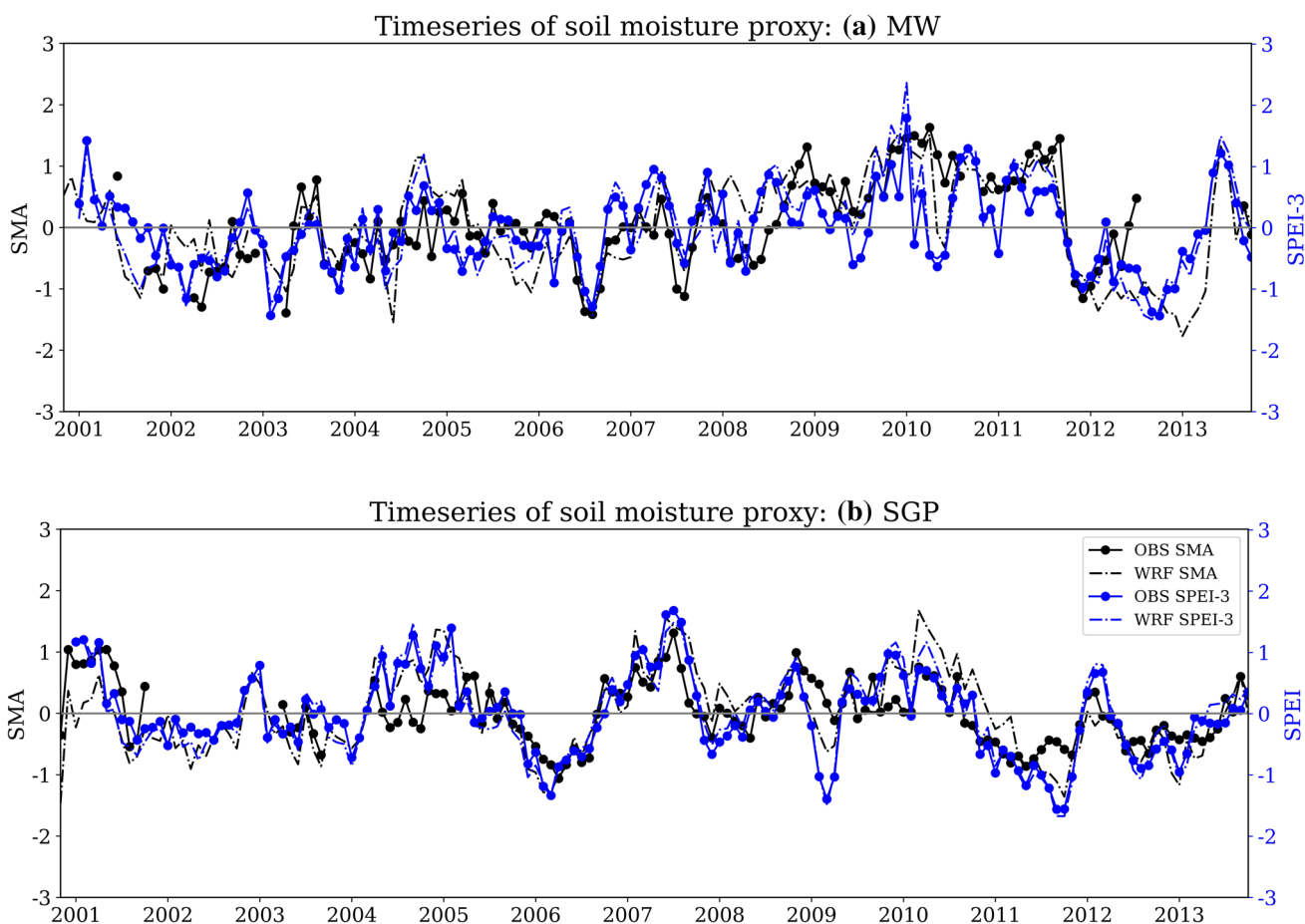


Fig. 4 Monthly soil moisture anomaly and SPEI-3 in selected two regions **a** in MW, and **b** in SGP. Solid dotted lines are from observational results, and dashed lines are from WRF model; black lines are for soil moisture anomaly and blue lines are for SPEI-3 index

Table 1 Pearson correlation coefficient between monthly timeseries of soil moisture anomaly and SPEI-3, from both observation and WRF model in two regions (MW and SGP)

Region	SMA_obs vs SMA_wrf	SMA_obs vs SPEI_obs	SPEI_obs vs SPEI_wrf	SMA_wrf vs SPEI_wrf
MW	0.706	0.546	0.905	0.762
SGP	0.692	0.716	0.965	0.826

Bold numbers indicate statistical significance with p value less than 0.01

summer heatwaves in most regions, including the South Great Plains (North Texas, Oklahoma, Kansas, Nebraska), Midwest (Wisconsin, Illinois, Iowa, Minnesota) and Gulf Coast (Louisiana, Arkansas, Mississippi). The WRF simulation shows less areas with statistical significance in the Canadian Prairies and Central US and more significant in Michigan ($p < 0.01$). These regions with significant anti-correlations resemble the land–atmosphere coupling “hot spots” in previous studies (Koster et al. 2004, 2006; Guo

et al. 2006). In these regions the antecedent soil moisture has strong influence on both frequency and magnitude of HWs and, thus, may possess some predictability for HWs, especially in the Midwest, South Great Plains, and Gulf Coast.

3.3 Quantile regression analysis

The purpose of introducing quantile regression is to show how antecedent soil moisture impacts on the two HW indices varies across different quantiles. The regression slope of antecedent soil moisture (expressed as SPEI-3) and HW indices represents the differences in the effects of soil moisture at various quantiles. Figures 6 and 7 show the spatial distribution of regression slopes for three quantiles (0.1, 0.5 and 0.9 for low, median and high quantile) of HWF and HWM against antecedent soil moisture (SPEI-3) for both observation (a–c) and WRF (d–f). The impacts of soil moisture deficits on HWF become stronger from the lower to the upper end of HWF distribution (Fig. 6a–c) and are prominently negative for 0.9 quantile (Fig. 6c, f). For the lower quantile (Fig. 6a, d) the regression slopes are close to zero

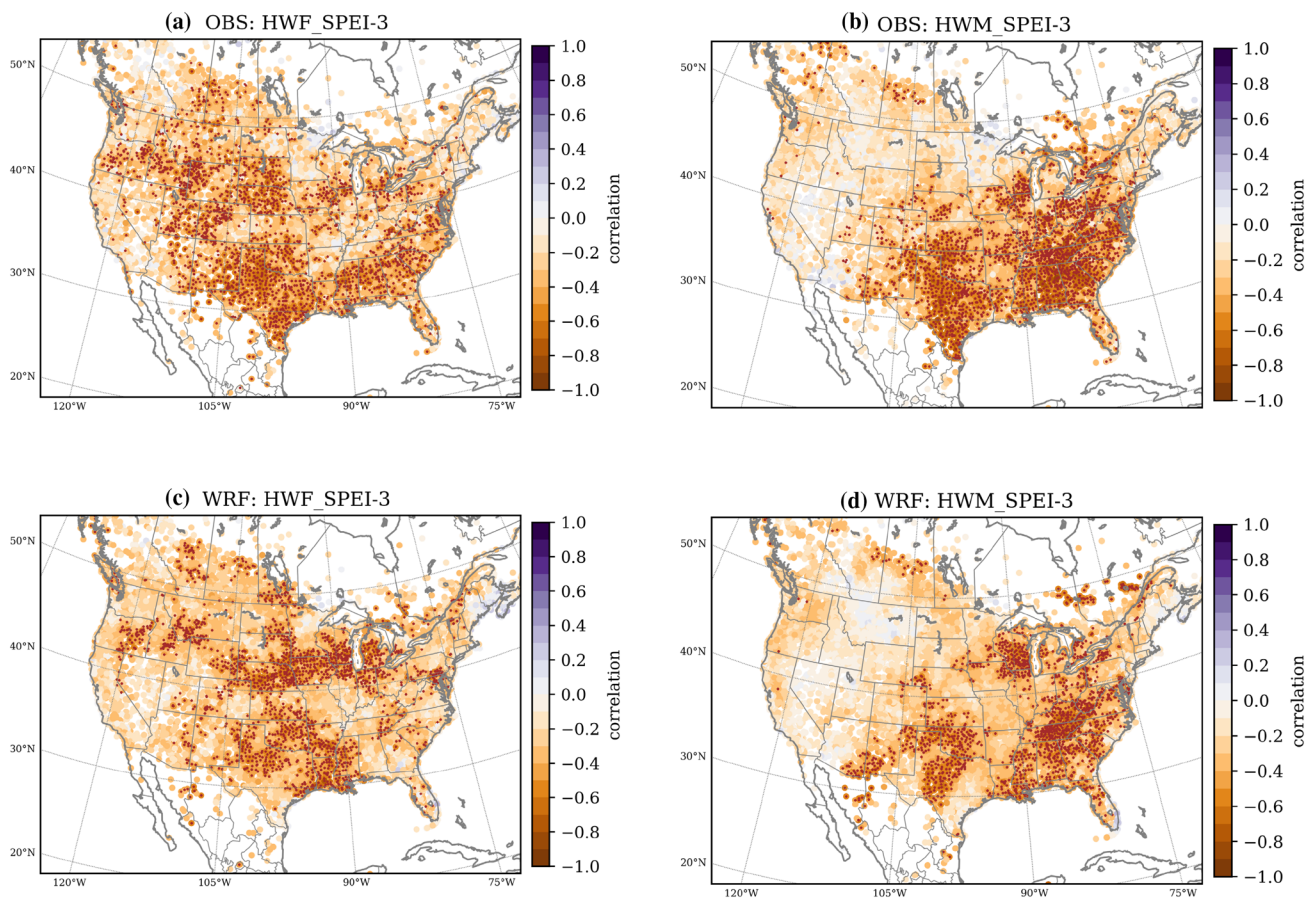


Fig. 5 Pearson's correlation coefficient between SPI-3 and HWF (**a**, **c**) and HWM (**b**, **d**), from observation (**a**, **b**) and WRF model (**c**, **d**). High-lighted stations/grid points indicate significant correlations at the 99% confidence level

across the domain. For the higher quantile (Fig. 6c, f), the strongest impacts of antecedent soil moisture on HWF are in the Midwest, South Great Plains and along the Gulf Coast, where significant anti-correlations are shown in Fig. 5a, c too. These results show that antecedent soil moisture has strong impacts on HWF, especially on the higher quantile, and can be used as a predictive index in these regions.

Unlike HWF, HWM exhibits strong relationships with antecedent soil moisture in the low quantile, which is most obvious in the South Great Plains and Pacific Northwest. It implies that antecedent soil moisture has a stronger impact on the low quantile HWM than the high quantile in these regions. The strong impacts of antecedent soil moisture on low HWM are accurately simulated in SGP region in WRF compared to that of the observations. However, antecedent soil moisture impacts on the higher quantiles (0.5 and 0.9 quantile) are underestimated. Quantile regression slopes in this region become smaller in WRF simulation than in the observations. There are also some regions, where strong relationship between SPEI-3 and HWM in all quantiles is seen, for example in the MW region. The

correlation becomes even stronger towards the high quantiles. Conversely, the WRF model simulate stronger impacts of antecedent soil moisture for the high quantiles than the observations in the MW region.

The heatwave indices in two regions, Midwest (MW) and South Great Plains (SGP), are analyzed further. For these two regions, the scatter plots of both HWF and HWM against SPEI-3 derived from observation and WRF simulation are shown in Fig. 8. The regression lines for five different quantiles (0.1, 0.3, 0.5, 0.7, 0.9) are overlaid with different colors. For HWF (Fig. 8a, c), in both regions observation shows a decreasing trend of regression slopes towards higher quantile with the slope values becoming more negative, which suggests a stronger impact of antecedent soil moisture on high HWF occurrence.

But for HWM, the scatter plots and quantile regression for these two regions show different features. In MW (Fig. 8c, d), although the trends of five regression lines are not as clear as that of HWF, it does show stronger impacts (with steeper slope) of antecedent soil moisture on high quantile (Fig. 8c) in both the WRF simulation and observation. On

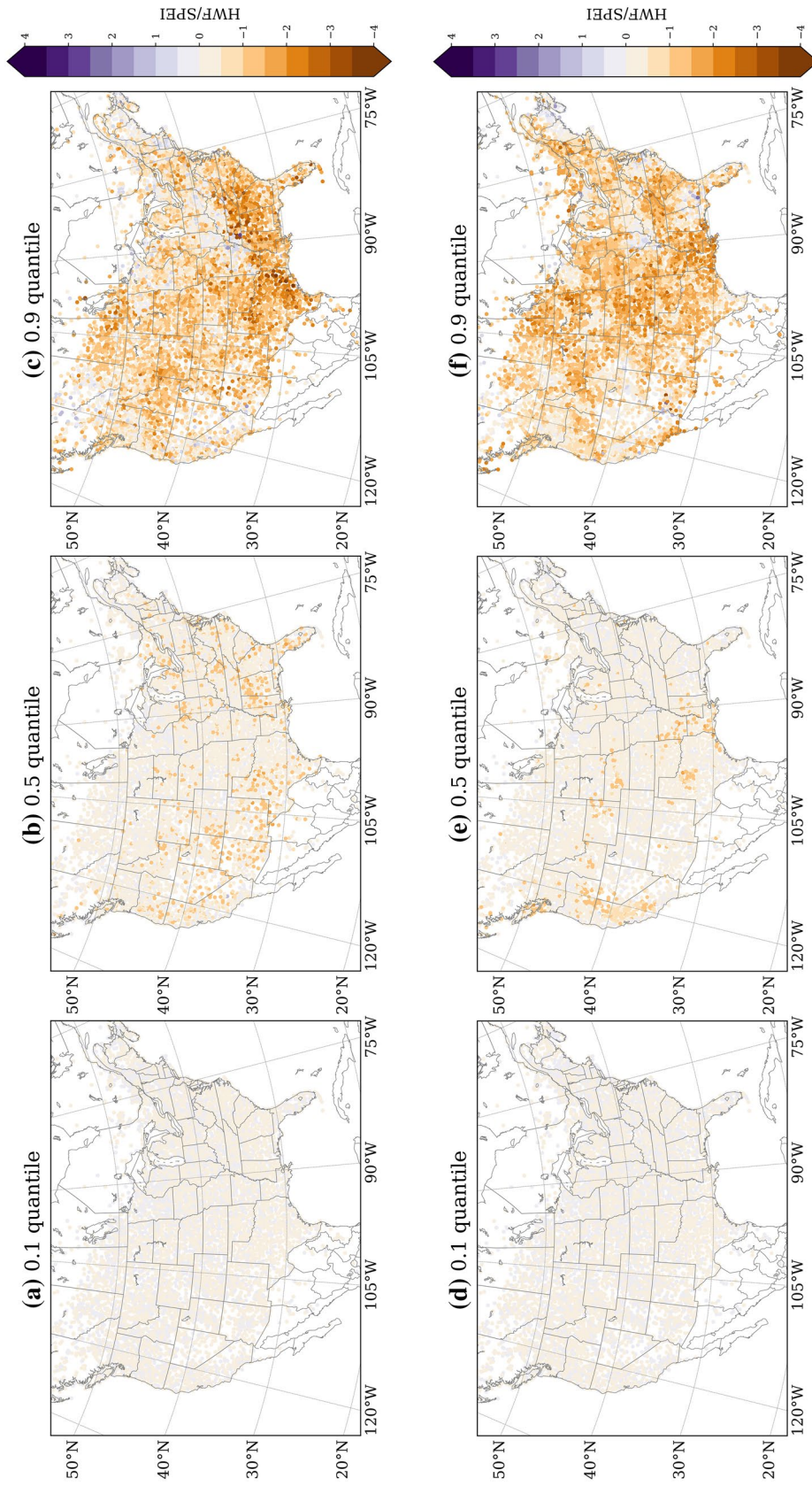


Fig. 6 Quantile regression slope between SPEI-3 and HWF at three quantiles, 0.1, 0.5 and 0.9, for low, median and high quantiles in OBS (a–c) and WRF (d–f)

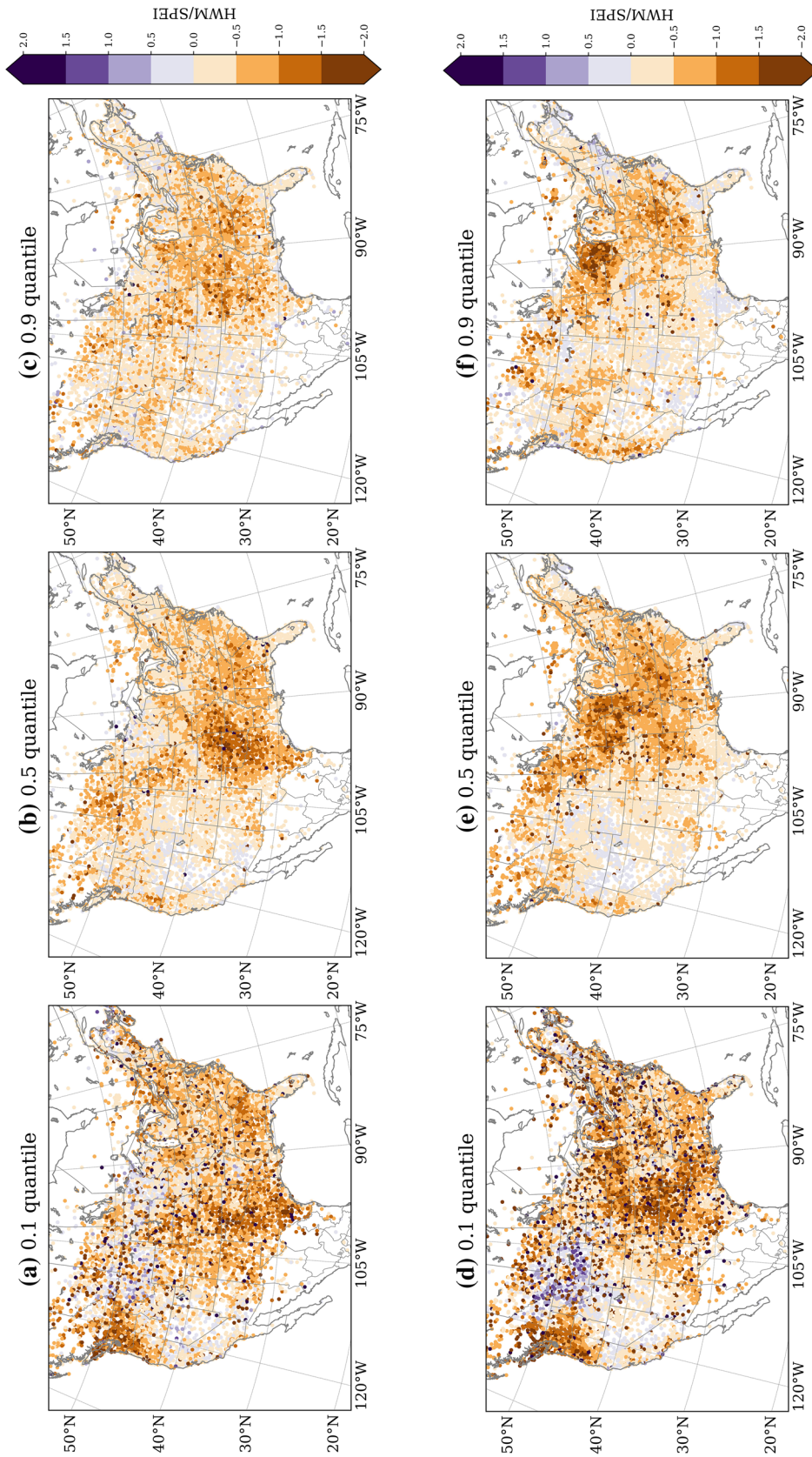


Fig. 7 Same as Fig. 6, but for quantile regression slope between SPEI-3 and HWM in OBS (a–c) and WRF (d–f)

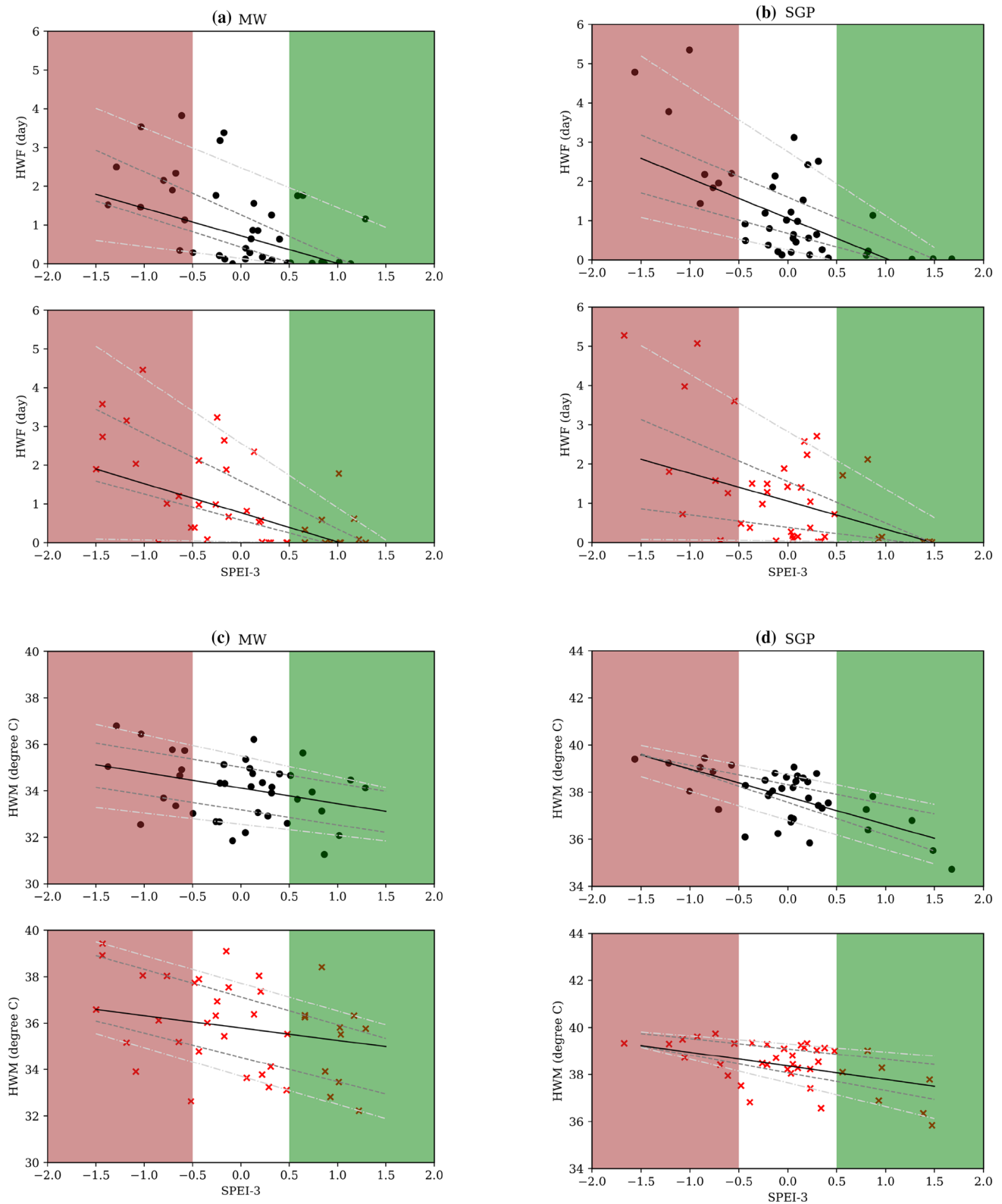


Fig. 8 Scatter plots of monthly HWF (**a, b**) and HWM (**c, d**) against SPEI-3 from high-density observation (top) and from WRF simulation (bottom), based on stations/grid points averaged values for Midwest (MW) (**a, c**) and South Great Plains (SGP) (**b, d**). Regression

lines for five different quantiles (0.1, 0.3, 0.5, 0.7 and 0.9) are shown with different colors. SPEI value larger (less) than 0.5 (-0.5) are shaded in green (brown) to distinguish abnormal wet (dry) condition

the contrary, in SGP, the regression slopes are flat for the 0.9 quantile and steep for the 0.1 quantile, indicating stronger impacts of soil moisture on lower quantiles (less negative) as shown in Fig. 8d.

The difference in HWM responses at various quantiles in two regions can be attributed to their different evaporation or soil moisture regimes (Schwingshackl et al. 2017). MW belongs to transitional-to-wet or transitional-to-energy limited evaporation regime. Summer precipitation amount is close to its potential evapotranspiration, so the region relies on moisture storage from last spring and winter as well as moisture input from current summer (Quiring and Klaver 2009). Thus, the occurrence and intensity of summer heatwaves rely on its antecedent soil moisture and summer weather condition. The dependence becomes even stronger for the high quantile of HWF and HWM. But SGP belongs to dry-to-transitional or soil moisture limited-to-transitional evaporation regime. Summer potential evapotranspiration is much stronger than precipitation. Summer convective weather in this region is more related to the moisture input, which is usually associated with the low-level jet as part of North Atlantic Subtropical High (NASH) that brings

moisture from Gulf of Mexico, but is less related to antecedent moisture storage in the soil. Thus, the high intensity heatwave events are more a response to summer weather condition than to antecedent soil moisture condition. Nonetheless, all three drivers including the summer weather conditions, antecedent dry soil moisture and anomalous SSTs induced by climate variability will contribute to the occurrence of intensive HW events in SGP (Hoerling et al. 2013).

To evaluate WRF model performance, the quantile regression slope between antecedent soil moisture and HWF/HWM were calculated from both observations and WRF simulation. Figure 9 shows the regression slopes of 9 quantiles for both HWF and HWM in MW and SGP, with the shaded area representing the 95% confidence interval. The decreasing trends (slopes getting more negative for higher quantile) of HWF and SPEI-3 in both regions are accurately simulated by WRF, except for high (low) quantiles in MW (SGP), where the WRF model overestimated (underestimated) the effect of antecedent soil moisture. For HWM, the decreasing trend in MW is not as obvious as that in SGP, given a large spread in the confidence interval; and an overestimation (underestimation) of the effects of

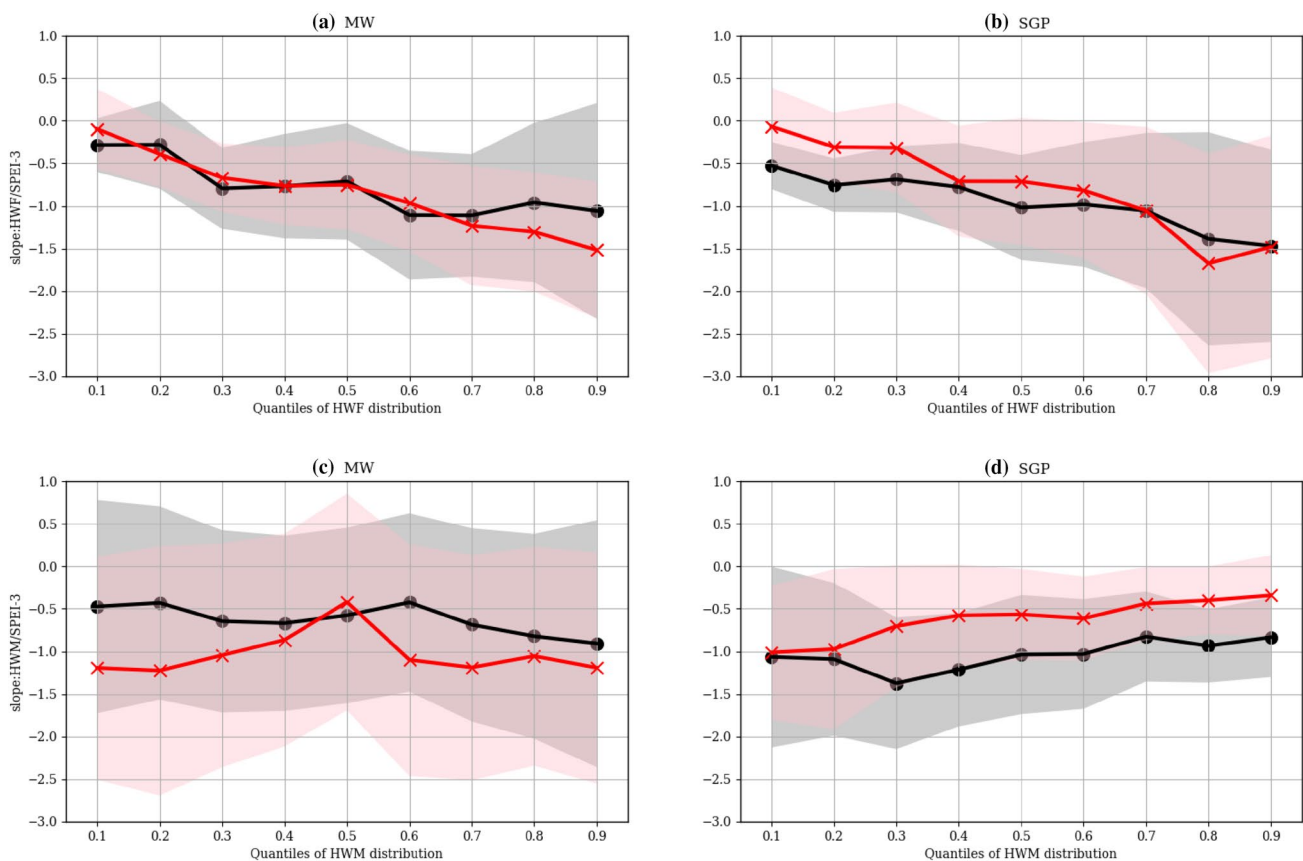


Fig. 9 Quantile regression slopes of the 0.1–0.9 quantiles for HWF (a, b) and HWM (c, d) in relation to SPEI-3 for the two regions (a, c: MW, b, d: SGW), for both OBS (black dot) and WRF (red cross).

The shaded areas are the 95% confidence interval for quantile regression slopes for each given quantile

antecedent soil moisture in MW (SGP) is shown for almost all quantiles. These two features are consistent with the spatial distribution of slopes shown in Fig. 7c–f.

4 Discussion

Multiple physical drivers exist behind heatwaves and the contribution of each driver may vary across events and regions. In a recent review paper on heatwaves by Perkins (2015), the physical drivers of HWs are summarized in three main categories: synoptic condition, soil moisture and land surface interaction, and climate variability. Our study focuses on the impacts of antecedent soil moisture on HWs through soil moisture-temperature feedback. The results show that the feedback is stronger in a transitional regime, while its manifestation requires interacting with other drivers.

For example, soil moisture variation shows little impacts on low quantile HWF in two focus regions, suggesting synoptic conditions may be more important for regions with insufficient surface energy, which would prohibit evapotranspiration regardless soil moisture condition (Li et al. 2018) (Figs. 6a, d, 8a, b). But for high quantile HWF, which are likely associated with anticyclonic static synoptic condition, antecedent soil moisture becomes a critical driver, amplifying the soil moisture feedback after dry spring but suppressing it when spring wet. This result about HWF is consistent with other studies using observational data from Europe and the globe (Hirschi et al. 2011; Herold et al. 2016; Mueller and Seneviratne 2012).

On the other hand, the quantile regression between SPEI-3 and HWM show different results. In SGP, where antecedent soil moisture has stronger impacts on low quantile HWM (Fig. 8d), the result is similar to a quantile regression study conducted for North and East part of Australia (Herold et al. 2016), which is also in dry regime in summer. However, in MW the antecedent soil moisture shows strong impacts on HWM in all quantiles (Fig. 8c), suggesting antecedent soil moisture is very important for HWM in this region.

Furthermore, the asymmetric response of HWF/HWM to antecedent soil moisture for different quantiles suggests potential predictive skill based on antecedent soil moisture condition, especially for high quantile of HWF in both focus regions and low quantile of HWM in SGP. This is described as “asymmetric predictability” by Quesada et al. (2012), who found that the occurrence of summer extreme heat events is more sensitive to certain weather regime after dry winter/spring compared to a wet season. Our results extend the conclusion to the magnitude of summer heatwaves, which depends more on synoptic weather systems in SGP

under wet soil condition, while the predictive skill of high HWM with dry soil is always high.

The different responses of HWM on different quantiles to antecedent soil moisture in these two regions (MW and SGP) could be explained by their different evaporation regimes and weather regimes in summer (Fig. 8c, d). In the summer in SGP, evaporation is moisture-limited and the synoptic conditions are largely dependent on the activities of the static anticyclonic high pressure systems North Atlantic Subtropical High, which brings moisture from Gulf of Mexico. Thus, antecedent soil moisture has stronger influence on low quantile of HWM, while synoptic conditions are a more dominant factor for the high quantile of HWM. On the contrary, summer precipitation in the MW depends largely on antecedent rainfall/snowfall in previous spring/winter. In this region, the moisture recycling through soil moisture-precipitation feedback (Li et al. 2017) confirms that it is in energy-limited-to-transitional regime. That explains why antecedent soil moisture is important for all quantiles of HWM (Fig. 8c), and a strengthening trend is observed towards higher quantiles (Fig. 9c).

In the relationship between antecedent soil moisture and summer HW indices, the biggest differences between WRF simulation and observation found in Figs. 6, 7, 8 and 9 could be explained by warm temperature bias and dry precipitation bias in both regions (Liu et al. 2017). In the MW, where summer precipitation relies on local moisture recycling, less precipitation and higher summer temperature introduce dry bias in soil moisture, higher evaporation demand further desiccating soil under the dry condition. This over-coupling between land and atmosphere contributes to a systematic overestimation of the impact of antecedent soil moisture on HWM in the MW (Figs. 7e, f, 9c). On the other hand, the warm bias and dry bias in SGP is more related to the activities of NASH, which is the dominant factors for the summer weather in SGP. Thus, the contribution of antecedent soil moisture to HWM is underestimated with less negative slope value in Figs. 7e, f and 9d.

Despite the warm and dry bias in the central US in summer have limited the model performance on HW magnitude, the WRF model accurately simulated the relationship between HW frequency and SPEI-3 in both regions. Other studies, comparing regional climate simulations with observations, found overestimation of the impacts of antecedent soil moisture deficits in wet regime (Hirschi et al. 2011). Our results showed reasonable estimation of soil moisture impacts on HW occurrence. This could be due to the improved representation of land surface properties in high-resolution model as well as the explicit simulation of convection in the model.

Although warm bias (3–4 °C) in daily maximum temperature exhibited in central US is a challenging issue in CPM simulation, our results showed considerable improvement

in simulated precipitation compared to coarser-resolution non-convection-permitting regional climate model in North America (Whan and Zwiers 2016). In addition, efforts in the Hydrometeorology Applications Program group in NCAR/RAL are being undertaken to reduce the warm and dry biases in this region. This study showed a statistical approach of evaluating the relationship between antecedent soil moisture and temperature, which contributes to the knowledge of antecedent soil moisture's impacts on HW aspects, the asymmetric predictive skill towards HWF/HWM and the diagnosis of land-atmosphere coupling in regional climate models.

5 Conclusion

Antecedent soil moisture has significant impacts on summer heatwaves, as it can amplify the frequency and intensity of heatwaves. Thus, it is essential to understand the physical mechanism behind soil moisture and heatwaves and evaluate how this relationship is represented in current regional climate model. This study investigates the impacts of spring soil moisture on summer heatwaves from station observations and the WRF regional climate model in convection-permitting configuration (WRF CONUS). We started with evaluating the 90th percentile of the daily maximum temperature in June–July–August (JJA), and used it as the threshold for defining heatwave events (TX90). The SPEI-3 is used as a proxy for 3-month antecedent soil moisture as the supplement to meteorological station soil moisture measurement. The WRF model simulated the spatial patterns of a statistical threshold temperature (TX90) of heatwaves reasonably well, except for a 3–4 °C of warm bias in Midwest and 2–3 °C of cold bias in western mountainous regions. Despite the high temperature bias in central US in WRF CONUS, the frequency and magnitude of HWs are reasonably simulated by WRF CONUS compared to the observation, when using a statistical threshold to define HW events (TX90). A soil moisture proxy, SPEI-3, is then evaluated against in-situ soil moisture measurement and the results showed that SPEI-3 is a good indicator for monthly soil moisture anomaly.

The soil moisture-temperature feedback is represented by anti-correlations between antecedent soil moisture, the SPEI-3, and two HW indices, HWF and HWM across the domain. These strong anti-correlations are significant over many areas in the North America, including the Midwest, North and South Great Plains, South Coast as well as the Canadian Prairie. The spatial distribution of these strong coupling regions has been captured reasonably by the WRF model.

Quantile regression analysis shows that the impacts of antecedent soil moisture are asymmetric for the occurrence and magnitude of HWs. The quantile regression slopes

represent the strength of the impact of soil moisture on HWF and HWM for different quantiles. For HWF, soil moisture has stronger impacts on the higher quantiles of the HWF, suggesting other have a larger effect in certain regions with sufficient surface energy, such as where anticyclonic synoptic conditions may play a dominant role. On the other hand, the asymmetric effect of soil moisture on HWM varies spatially. For two regions in interest, the Midwest (MW) and South Great Plains (SGP), the impacts of antecedent soil moisture are stronger for the lower quantile of HWM in SGP, while strong for all the quantiles in MW. This difference could be related to their different summer weather regimes - summer weather in SGP is highly impacted by large synoptic scale processes, while in MW it is largely depended on local feedback through moisture recycling of the antecedent rain/snowfall.

The asymmetric response of heatwave occurrence and magnitude to antecedent soil moisture (stronger for higher quantiles of HWF in both regions but for lower quantiles of HWM in SGP) provide important information for the improvement of their predictive skill, as it is confident that less heatwave events and lower heatwave temperatures will appear after a wet spring than a dry spring in two regions. In SGP, antecedent dry soil moisture embedded higher predictability for high HWM while less predictability for high HWF.

The WRF model also represents well the regression slopes for HWF in most of the quantiles in both regions, but overestimates the slopes for HWM in MW and underestimates the slopes in SGP. The warmer temperature and less precipitation bias in these two regions in summer led to increased evaporative demands and further desiccated soil moisture, hence, strengthened local feedback in the MW. On the other hand, other processes might be responsible for underestimated land-atmosphere coupling in SGP, such as the activities of NASH. Overall, the WRF CONUS simulation is capable of capturing the soil moisture-temperature feedbacks in these two regions, which has strong connection in summer heatwaves.

The role of soil moisture in land-atmosphere interaction, particularly in heatwaves are complicated and need further analysis. Our study has important implications for land-atmosphere coupling research as well as heatwave monitoring and forecasting. Here we list a few non-exhaustive implications as well as our future research plan:

1. Predictive skill for agriculture activities: agriculture is very important but highly diverse in both regions, with the eastern part of MW and SGP mainly rain-fed crop but western part irrigated. Rain-fed crop production, in particular, is critically dependent on weather conditions in the warm season. Extreme temperature-induced heat stress can seriously affect crop production. These two

regions are also major places for livestock production, including dairy and beef cattle, hogs and others, which are also sensitive to heatwaves.

2. Diagnosis on land–atmosphere coupling: the overestimation of soil moisture impacts on summer heatwaves in the MW regions, both seen in the high quantile of HWF and HWM, could be attributed to too strong land–atmosphere coupling. There have been many theories regarding the over-coupling issue, including too strong surface coupling due to out-of-date assumption on short vegetation in this region, which are mainly crop and grassland, which transport higher heat flux from the surface to the atmosphere, hence, intensifying the soil moisture–temperature feedback. (Chen et al. 1997; Chen and Zhang 2009). Another theory is related to lack of irrigation over this region in the land surface model, where irrigation water could be a significant input that increases soil moisture and evapotranspiration and cools the air (Huber et al. 2014). These are strong motivations and potentials for future land–atmosphere coupling studies.
3. High resolution convection permitting model: the initial motivation of performing high resolution regional climate modeling is its advantages in simulating convective precipitation. However, a recent study on the summer convection storms using the same model data showed less convection population simulated in the current climate than observation (Rasmussen et al. 2017). This result is connected to our findings here that a warm and dry bias in the Great Plain region amplify soil moisture–temperature feedback while suppress soil moisture–precipitation feedback. The diagnosis and improvement of land–atmosphere coupling in regional climate model can potentially benefit the performance of convection-permitting regional climate model.
4. Climate change impacts on land–atmosphere coupling: In the second part of the WRF CONUS simulation, a Pseudo Global Warming (PGW) method is applied to add a climate perturbation from RCP8.5 scenario to current climate, implying global warming. How global warming impacts on land–atmosphere coupling, particularly how soil moisture could impact heatwaves in future climate, could be an interesting research topic.

Heatwaves are extreme temperature events that has disastrous effects on human health and societies. Thus, it is important to understand the physical mechanism of soil moisture, and its interaction with synoptic condition and climate variability and how they relate to HWs. This can provide useful information for heatwave forecast and mitigation approaches.

Acknowledgements The authors Zhe Zhang, Yanping Li, Zhenhua Li gratefully acknowledge the support from the Changing Cold Regions

Network (CCRN) funded by the Natural Science and Engineering Research Council of Canada (NSERC), as well as the Global Water Future project and Global Institute of Water Security at University of Saskatchewan. Yanping Li acknowledge the support from NSERC Discovery Grant. Fei Chen, Michael Barlage appreciate the support from the Water System Program at the National Center for Atmospheric Research (NCAR), USDA NIFA Grants 2015-67003-23508 and 2015-67003-23460, and NSF Grant #1739705. NCAR is sponsored by the National Science Foundation. Any opinions, findings, conclusions or recommendations expressed in this publication are those of the authors and do not necessarily reflect the views of the National Science Foundation.

References

- Barlage M, Tewari M, Chen F, Miguez-Macho G, Yang ZL, Niu GY (2015) The effect of groundwater interaction in North American regional climate simulations with WRF/Noah-MP. *Clim Change* 129(3–4):485–498. <https://doi.org/10.1007/s10584-014-1308-8>
- Brooke Anderson G, Bell ML (2011) Heat waves in the United States: mortality risk during heat waves and effect modification by heat wave characteristics in 43 US communities. *Environ Health Perspect* 119(2):210–218. <https://doi.org/10.1289/ehp.1002313>
- Cai X, Yang ZL, David CH, Niu GY, Rodell M (2014a) Hydrological evaluation of the noah-MP land surface model for the Mississippi River Basin. *J Geophys Res* 119(1):23–38. <https://doi.org/10.1002/2013JD020792>
- Cai X, Yang ZL, Xia YL, Huang M, Wei H, Leung LR (2014b) Assessment of simulated water balance from Noah, Noah-MP, CLM, and VIC over CONUS using the NLDAS test bed. *J Geophys Res Atmos* 119:1–20. <https://doi.org/10.1002/2014JD022113>
- Chen F, Dudhia J (2001) Coupling an advanced land surface—hydrology model with the Penn State—NCAR MM5 modeling system. Part I: model implementation and sensitivity. *Mon Weather Rev*. [https://doi.org/10.1175/1520-0493\(2001\)129](https://doi.org/10.1175/1520-0493(2001)129)
- Chen F, Zhang Y (2009) On the coupling strength between the land surface and the atmosphere. *Geophys Res Lett* 36:L10404. <https://doi.org/10.1029/2009GL037980>
- Chen F, Janjic ZI, Mitchell K (1997) Impact of atmospheric surface-layer parameterizations in the new land-surface scheme of the NCEP mesoscale eta model. *Bound Layer Meteorol* 85:391–421. <https://doi.org/10.1023/A:1000531001463>
- Chen F, Liu C-H, Dudhia J, Chen M (2014) A sensitivity study of high-resolution regional climate simulations to three land surface models over the western United States. *J Geophys Res* 119:7271–7291. <https://doi.org/10.1002/2014JD021827>
- Dai A (2011) Drought under global warming: a review. *Wiley Interdiscip Rev Clim Change* 2(1):45–65. <https://doi.org/10.1002/wcc.81>
- Diffenbaugh NS, Ashfaq M (2010) Intensification of hot extremes in the United States. *Geophys Res Lett* 37(15):1–5. <https://doi.org/10.1029/2010GL043888>
- Duda JD, Wang X, Xue M (2017) Sensitivity of convection-allowing forecasts to land surface model perturbations and implications for ensemble design. *Mon Weather Rev* 145(5):2001–2025. <https://doi.org/10.1175/MWR-D-16-0349.1>
- Durre I, Wallace JM, Lettenmaier DP (2000) Dependence of extreme daily maximum temperatures on antecedent soil moisture in the contiguous United States during summer. *J Clim* 13(14):2641–2651
- Fischer EM, Seneviratne SI, Vidale PL, Lüthi D, Schär C (2007) Soil moisture–atmosphere interactions during the 2003 European summer heat wave. *J Clim* 20(20):5081–5099. <https://doi.org/10.1175/JCLI4288.1>

- Guo Z et al (2006) GLACE: the global land–atmosphere coupling experiment. Part II: analysis. *J Hydrometeorol* 7(4):611–625. <https://doi.org/10.1175/JHM511.1>
- Hauser M, Orth R, Seneviratne SI (2015) Role of soil moisture vs. recent climate change for heat waves in western Russia. *Geophys Res Lett* 43(10):2819–2826. <https://doi.org/10.1002/2016GL068036>. Received
- Herold N, Kala J, Alexander LV (2016) The influence of soil moisture deficits on Australian heatwaves. *Environ Res Lett* 11(6):64003. <https://doi.org/10.1088/1748-9326/11/6/064003>
- Hirschi M et al (2011) Observational evidence for soil-moisture impact on hot extremes in southeastern Europe. *Nat Geosci* 4(1):17–21. <https://doi.org/10.1038/ngeo1032>
- Hoerling M et al (2013) Anatomy of an extreme event. *J Clim* 26(9):2811–2832. <https://doi.org/10.1175/JCLI-D-12-00270.1>
- Hong S-Y, Noh Y, Dudhia J (2006) A new vertical diffusion package with an explicit treatment of entrainment processes. *Mon Weather Rev* 134:2318–2341
- Huber D, Mecham D, Brunsell N (2014) The effects of Great Plains irrigation on the surface energy balance, regional circulation, and precipitation. *Climate* 2(2):103–128. <https://doi.org/10.3390/cli2020103>
- Iacono MJ, Delamere JS, Mlawer EJ, Shephard MW, Clough SA, Collins WD (2008) Radiative forcing by long-lived greenhouse gases: calculations with the AER radiative transfer models. *J Geophys Res* 113:D13103. <https://doi.org/10.1029/2008JD009944>
- IPCC (2012) Managing the risks of extreme events and disasters to advance climate change adaptation. In: Field CB, Barros V, Stocker TF, Qin D, Dokken DJ, Ebi KL, Mastrandrea MD, Mach KJ, Plattner G-K, Allen SK, Tignor M, Midgley PM (eds) A special report of working groups I and II of the intergovernmental panel on climate change. Cambridge University Press, Cambridge, p 582
- Jaeger EB, Seneviratne SI (2011) Impact of soil moisture–atmosphere coupling on European climate extremes and trends in a regional climate model. *Clim Dyn* 36(9–10):1919–1939. <https://doi.org/10.1007/s00382-010-0780-8>
- Koster RD, Guo Z, Bonan G, Chan E, Cox P (2004) Regions of strong coupling between. *Science* 1138(2004):10–13. <https://doi.org/10.1126/science.1100217>
- Koster RD et al (2006) GLACE: the global land–atmosphere coupling experiment. Part I: overview. *J Hydrometeorol* 7(4):590–610. <https://doi.org/10.1175/JHM510.1>
- Koster RD, Schubert SD, Suarez MJ (2009) Analyzing the concurrence of meteorological droughts and warm periods, with implications for the determination of evaporative regime. *J Clim* 22(12):3331–3341. <https://doi.org/10.1175/2008JCLI2718.1>
- Li YP et al (2017) A numerical study of the June 2013 flood-producing extreme rainstorm over Southern Alberta. *J Hydrometeorol* 18(8):2057–2078. <https://doi.org/10.1175/JHM-D-15-0176.1>
- Li ZH, Li YP, Bonsal B, Manson A, Scaff L (2018) Combined impacts of ENSO and MJO on the 2015 growing season drought over the Canadian Prairies. *Hydrol Earth Syst Sci Discuss.* <https://doi.org/10.5194/hess-2018-56>
- Liu CH et al (2017) Continental-scale convection-permitting modeling of the current and future climate of North America. *Clim Dyn* 49(1–2):71–95. <https://doi.org/10.1007/s00382-016-3327-9>
- Ma HY et al (2014) On the correspondence between mean forecast errors and climate errors in CMIP5 models. *J Clim* 27(4):1781–1798. <https://doi.org/10.1175/JCLI-D-13-00474.1>
- McKee TB, Doesken NJ, Kleist J (1993) The relationship of drought frequency and duration of time scales. Eighth conference on applied climatology, American Meteorological Society, Jan 17–23, 1993, Anaheim CA, pp 179–186
- Meehl GA, Tebaldi C (2004) More intense, more frequent, and longer lasting heat waves in the 21st century. *Science* 305(5686):994–997. <https://doi.org/10.1126/science.1098704>
- Meng L, Shen Y (2014) On the relationship of soil moisture and extreme temperatures in East China. *Earth Interact.* <https://doi.org/10.1175/2013EI000551.1>
- Menne MJ, Durre I, Vose RS, Gleason BE, Houston TG (2012) An overview of the global historical climatology network-daily database. *J Atmos Ocean Technol* 29(7):897–910. <https://doi.org/10.1175/JTECH-D-11-00103.1>
- Miralles DG, Teuling AJ, van Heerwaarden CC, Vilà-Guerau de Arellano J (2014) Mega-heatwave temperatures due to combined soil desiccation and atmospheric heat accumulation. *Nat Geosci* 7(5):345–349. <https://doi.org/10.1038/ngeo2141>
- Mueller B, Seneviratne SI (2012) Hot days induced by precipitation deficits at the global scale. *Proc Natl Acad of Sci* 109(31):12398–12403. <https://doi.org/10.1073/pnas.1204330109>
- Musselman KN, Clark MP, Liu CH, Ikeda K, Rasmussen R (2017) Slower snowmelt in a warmer world. *Nat Clim Change* 7(February):214–220. <https://doi.org/10.1038/NCLIMATE3225>
- Newman AJ et al (2015) Gridded ensemble precipitation and temperature estimates for the contiguous United States. *J Hydrometeorol* 16(6):2481–2500. <https://doi.org/10.1175/JHM-D-15-0026.1>
- Niu GY et al (2011) The community Noah land surface model with multiparameterization options (Noah-MP): 1. Model description and evaluation with local-scale measurements. *J Geophys Res Atmos* 116(12):1–19. <https://doi.org/10.1029/2010JD015139>
- Orlowsky B, Seneviratne SI (2013) Elusive drought: uncertainty in observed trends and short-and long-term CMIP5 projections. *Hydrol Earth Syst Sci* 17(5):1765–1781. <https://doi.org/10.5194/hess-17-1765-2013>
- Perkins SE (2015) A review on the scientific understanding of heatwaves—their measurement, driving mechanisms, and changes at the global scale. *Atmos Res* 164–165:242–267. <https://doi.org/10.1016/j.atmosres.2015.05.014>
- Perkins SE, Alexander LV (2013) On the measurement of heat waves. *J Clim* 26(13):4500–4517. <https://doi.org/10.1175/JCLI-D-12-00383.1>
- Prein AF, Gobiet A, Suklitsch M, Truhetz H, Awan N, Keuler K, Georgievski G (2013a) Added value of convection permitting seasonal simulations. *Clim Dyn* 41(9–10):2655–2677
- Prein AF, Holland GJ, Rasmussen RM, Done J, Ikeda K, Clark MP, Liu CH (2013b) Importance of regional climate model grid spacing for the simulation of heavy precipitation in the Colorado headwaters. *J Clim* 26(13):4848–4857
- Prein AF et al (2015) A review on regional convection-permitting climate modeling: demonstrations, prospects, and challenges. *Rev Geophys* 53(2):323–361
- Quesada B, Vautard R, Yiou P, Hirschi M, Seneviratne SI (2012) Asymmetric European summer heat predictability from wet and dry southern winters and springs. *Nat Clim Change* 2(10):736–741. <https://doi.org/10.1038/nclimate1536>
- Quiring SM, Kluver DB (2009) Relationship between winter/spring snowfall and summer precipitation in the Northern Great Plains of North America. *J Hydrometeorol* 10(5):1203–1217. <https://doi.org/10.1175/2009JHM1089.1>
- Rasmussen KL, Prein AF, Rasmussen RM, Ikeda K, Liu C (2017) Changes in the convective population and thermodynamic environments in convection-permitting regional climate simulations over the United States. *Clim Dyn.* <https://doi.org/10.1007/s00382-017-4000-7>
- Schaefer GL, Cosh MH, Jackson TJ (2007) The USDA natural resources conservation service soil climate analysis network (SCAN). *J Atmos Ocean Technol* 24(12):2073–2077. <https://doi.org/10.1175/2007JTECHA930.1>

- Schwingshackl C, Hirschi M, Seneviratne SI (2017) Quantifying spatiotemporal variations of soil moisture control on surface energy balance and near-surface air temperature. *J Clim* 30(18):7105–7124. <https://doi.org/10.1175/JCLI-D-16-0727.1>
- Seneviratne SI, Lüthi D, Litschi M, Schär C (2006) Land–atmosphere coupling and climate change in Europe. *Nature* (443(7108):205–209. <https://doi.org/10.1038/nature05095>
- Seneviratne SI et al (2010) Investigating soil moisture–climate interactions in a changing climate: a review. *Earth Sci Rev* 99(3–4):125–161. <https://doi.org/10.1016/j.earscirev.2010.02.004>
- Skamarock WC et al (2008) A description of the advanced research WRF Version 3. NCAR Technical Note NCAR/TN-475 + STR. <https://doi.org/10.5065/D68S4MVH>
- Sun Q, Miao C, AghaKouchak A, Duan Q (2017) Unraveling anthropogenic influence on the changing risk of heat waves in China. *Geophys Res Lett* 44(10):5078–5085. <https://doi.org/10.1002/2017GL073531>
- Thompson G, Eidhammer T (2014) A study of aerosol impacts on clouds and precipitation development in a large winter cyclone. *J Atmos Sci* 71:3636–3658
- Thornthwaite CW (1948) An approach toward a rational classification of climate. *Geogr Rev* 38(1):55–94. [https://doi.org/10.1016/0022-3115\(71\)90076-6](https://doi.org/10.1016/0022-3115(71)90076-6)
- Vicente-Serrano SM, Beguería S, López-Moreno JI (2009) A multi-scalar drought index sensitive to global warming: the standardized precipitation evapotranspiration index. *J Clim*. <https://doi.org/10.1175/2009JCLI2909.1>
- Whan K, Zwiers F (2016) Evaluation of extreme rainfall and temperature over North America in CanRCM4 and CRCM5. *Clim Dyn* 46(11–12):3821–3843. <https://doi.org/10.1007/s00382-015-2807-7>
- Whan K et al (2015) Impact of soil moisture on extreme maximum temperatures in Europe. *Weather Clim Extremes* 9:57–67. <https://doi.org/10.1016/j.wace.2015.05.001>
- Yang ZL, Niu GY, Mitchell KE, Chen F, Ek MB, Barlage M et al. (2011) The community Noah land surface model with multiparameterization options (Noah-MP): 2. Evaluation over global river basins. *J Geophys Res Atmos* 116(12):1–16. <https://doi.org/10.1029/2010JD015140>